Macromolecular Materials and Engineering

Open Access

Supporting Information

Development and Characterization of Poly(butylene succinate-*co*-adipate)/Poly(3-hydroxybutyrate-*co*-3-hydroxyvalerate) with Cowpea Lignocellulosic Fibers as a Filler via Injection Molding and Extrusion Film-Casting

Mondli Abednicko Masanabo, Amélie Tribot, Enni Luoma, Jussi Virkajärvi, Nusrat Sharmin, Morten Sivertsvik, Suprakas Sinha Ray, Janne Keränen and M. Naushad Emmambux*

Development and Characterization of Poly(butylene succinate-co-adipate)/Poly(3-hydroxybutyrate-co-3-hydroxyvalerate) with Cowpea Lignocellulosic Fibers as a Filler via Injection Molding and Extrusion Film-casting

Mondli Abednicko Masanabo, Amélie Tribot, Enni Luoma, Jussi Virkajärvi, Nusrat Sharmin, Morten Sivertsvik, Suprakas Sinha Ray, Janne Keränen, M. Naushad Emmambux[*]
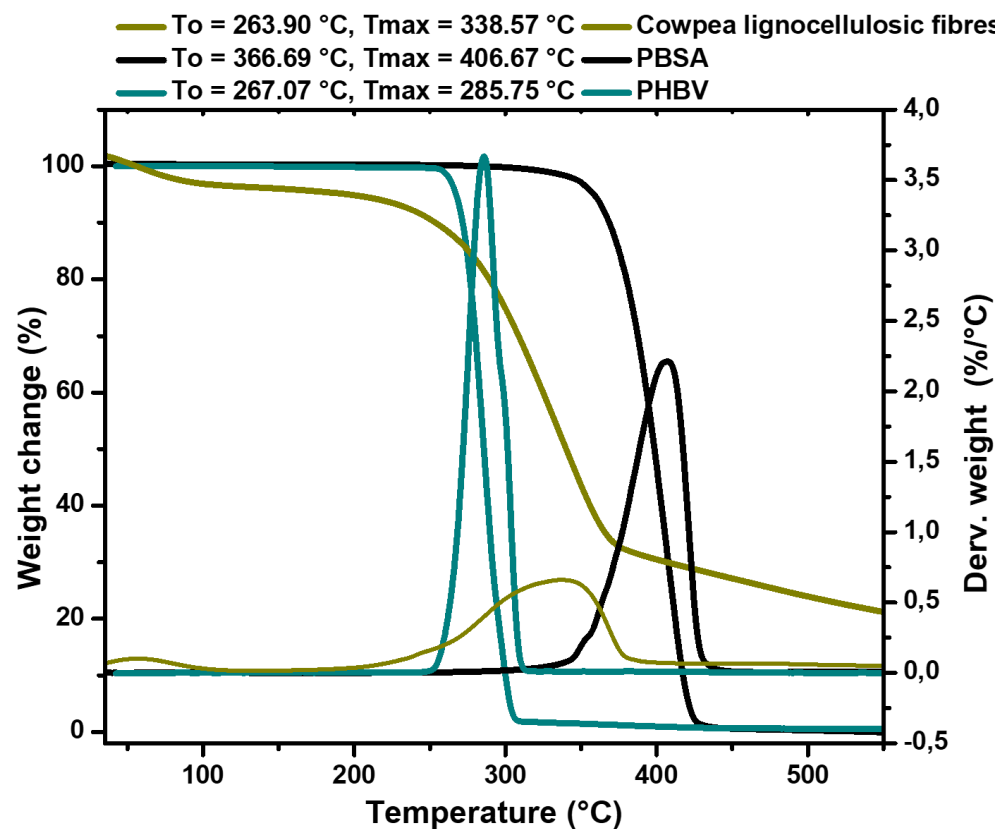
Figure S1: TGA (Y1) and derivative TGA (Y2) of PBSA, PHBV and cowpea lignocellulosic fibers.

Table S1: Thermal properties of injection molded bio-composites

| | TGA | | | | DMA | | DSC | | | | | | | | | |
| | | | | | PBSA | PHBV | PBSA | | | | | PHBV | | | | |
Samples	T_o (°C)	T_{max1} (°C)	T_{max2} (°C)	Residue mass (%)	T_{g1} (°C)	T_{g2} (°C)	T_{m1} (°C)	T_{m2} (°C)	ΔH_m (j/g)	X_c (%)	T_{c1} (°C)	T_{m1} (°C)	T_{m2} (°C)	ΔH_m (j/g)	X_c (%)	T_{c2} (°C)
PBSA/PHBV (85/15)	287.68 ± 1.02[b]	300.57 ± 3.50[b]	405.41 ± 2.95[a]	0.46 ± 0.03[a]	-36.58 ± 0.44[a]	6.08 ± 0.31[a]	73.07 ± 0.82[a]	86.97 ± 0.22[a]	43.60 ± 0.57[c]	45.24 ± 0.59[b]	46.38 ± 1.65[b]	168.64 ± 0.01[b]	173.37 ± 0.18[a]	12.42 ± 0.15[c]	56.69 ± 0.68[b]	94.90 ± 3.05[b]
PBSA/PHBV / 10 % CSS	270.09 ± 5.69[b]	283.27 ± 2.00[a]	400.14 ± 1.45[a]	1.76 ± 0.00[ab]	-34.46 ± 0.15[b]	7.26 ± 0.07[b]	71.17 ± 0.25[a]	86.99 ± 0.36[a]	36.50 ± 2.82[b]	42.07 ± 3.25[ab]	40.96 ± 0.36[a]	168.08 ± 0.03[b]	174.01 ± 0.44[a]	10.25 ± 0.78[c]	51.98 ± 3.98[a]	84.24 ± 1.57[a]
PBSA/PHBV / 20 % CSS	268.29 ± 2.34[b]	281.83 ± 0.03[a]	400.49 ± 1.45[a]	3.00 ± 0.00[bc]	-34.43 ± 0.33[b]	7.11 ± 0.02[b]	71.04 ± 0.21[a]	86.71 ± 0.25[a]	31.87 ± 2.31[ab]	41.34 ± 2.99[ab]	41.94 ± 0.40[a]	166.18 ± 0.25[a]	173.57 ± 0.30[a]	9.12 ± 0.54[ab]	51.72 ± 3.54[a]	85.08 ± 0.25[a]
PBSA/PHBV / 30 % CSS	257.01 ± 1.71[a]	281.50 ± 0.49[a]	399.14 ± 0.00[a]	4.88 ± 1.30[c]	-33.21 ± 0.01[c]	8.59 ± 0.22[c]	72.78 ± 0.54[a]	86.77 ± 0.30[a]	29.31 ± 0.05[a]	33.73 ± 0.06[a]	45.00 ± 0.07[b]	167.41 ± 0.81[ab]	174.08 ± 0.28[a]	7.88 ± 0.27[a]	51.34 ± 1.75[a]	82.96 ± 0.23[a]

Means followed by standard deviation. Means with different letters in the same column are significantly different ($p < 0.05$). T_o is the initial degradation temperature from TGA curve. T_g is the glass transition temperature from the DMA tan δ curve. T_{max} is the peak degradation temperature from the dTGA curve. T_m is the melting temperature, ΔH_m is the melting enthalpy from the DSC curve and X_c is the crystallinity of the polymers in the composites calculated from ΔH_m. T_c is the melt crystallization from the DSC cooling curve.

Table S2: Thermal properties of bio-composite films

| | TGA | | | | DMA | | DSC | | | | | | | | | |
| | | | | | PBSA | PHBV | PBSA | | | | | PHBV | | | | |
Samples	T_o (°C)	T_{max1} (°C)	T_{max2} (°C)	Residue mass (%)	T_{g1} (°C)	T_{g2} (°C)	T_{m1} (°C)	T_{m2} (°C)	ΔH_m (j/g)	X_c (%)	T_{c1} (°C)	T_{m1} (°C)	T_{m2} (°C)	ΔH_m (j/g)	X_c (%)	T_{c2} (°C)
PBSA/PHBV (85/15)	283.15 ± 0.23[d]	302.69 ± 3.50[b]	402.43 ± 2.74[a]	0.96 ± 0.33[a]	-39.69 ± 1.83[a]	0.76 ± 0.38[a]	75.49 ± 0.08[d]	86.05 ± 0.01[b]	48.97 ± 1.18[d]	50.97 ± 1.22[a]	53.22 ± 0.22[d]	168.08 ± 0.11[a]	172.64 ± 0.13[a]	14.55 ± 0.18[d]	65.84 ± 0.00[b]	92.99 ± 2.57[b]
PBSA/PHBV / 10 % CSS	270.98 ± 1.23[c]	282.56 ± 0.99[a]	399.52 ± 1.38[a]	1.79 ± 1.22[a]	-39.29 ± 0.03[a]	0.79± 0.03[a]	74.67 ± 0.03[c]	86.00 ± 0.08[b]	44.11 ± 0.20[c]	50.85 ± 0.22[c]	51.67 ± 0.16[c]	168.37 ± 1.30[a]	172.81 ± 0.04[ab]	12.09 ± 0.43[c]	61.31 ± 2.19[ab]	84.22 ± 0.74[a]
PBSA/PHBV / 20 % CSS	260.97 ± 1.42[b]	279.74 ± 0.99[a]	395.45 ±1.85[a]	2.99 ± 0.58[a]	-38.32 ± 0.82[a]	1.24 ± 0.01[ab]	72.74 ± 0.09[b]	85.75 ±0.05[ab]	35.94 ± 0.50[b]	45.95 ± 0.27[b]	47.37 ±0.03[b]	166.59 ± 0.36[a]	172.99 ± 0.02[bc]	10.49 ± 0.25[b]	59.85 ± 1.41[a]	82.09 ± 0.08[a]
PBSA/PHBV / 30 % CSS	254.26 ± 0.33[a]	277.97 ± 1.50[a]	398.03 ± 2.49[a]	3.54 ± 0.59[a]	-37.13 ± 2.17[a]	2.58 ± 0.70[b]	72.22 ± 0.11[a]	85.96 ± 0.08[a]	29.80 ± 0.93[a]	34.30 ± 1.07[a]	45.57 ± 0.25[a]	166.76 ± 0.02[a]	173.16 ± 0.09[c]	8.30 ± 0.42[a]	56.71 ± 0.92[a]	80.68 ± 1.09[a]

Means followed by standard deviation. Means with different letters in the same column are significantly different ($p<0.05$). T_o is the initial degradation temperature from TGA curve. T_g is the glass transition temperature from the DMA tan δ curve. T_{max} is the peak degradation temperature from the dTGA curve. T_m is the melting temperature, ΔH_m is the melting enthalpy from the DSC curve and X_c is the crystallinity of the polymers in the composites calculated from ΔH_m. T_c is the melt crystallization from the DSC cooling curve.

X-ray tomography image analysis

VTT in-house analysis software was used for the X-ray tomography image analysis. Part of this software is based on opensource software pi2 (process image 2) by A. Miettinen [1]. Below we describe the image preprocessing and image analysis steps and provide extra 3D visualizations of the samples.

Injection molded bio-composites

The 3D images were first cropped to include only a volume from inside the sample. 3D gaussian filter ($\sigma_i = 1$) was used to remove the small-scale noise and high pass filter (3D gaussian filter with $\sigma_i = 30$) was used to remove a large scale, beam hardening type, image artefact from the image. Different materials (matrix, cowpea, pores) where separated using grey value thresholding. After thresholding volume fraction of material, A was calculated in usual manner i.e. the number of voxels threshold as material A divided by the total number of voxels in the image. 3D visualizations of the dog bone samples are given in Figure S2.

Figure S2: 3D visualizations of the fibres in the injection moulded bio-composites containing (a) 10, (b) 20 and (c) 30% cowpea sidestream. Polymer matrix not included, i.e. transparent.

Bio-composite films

In the bio-film images sample surface region seemed to have non-physical image artefact (possible some sort of phase-contrast or diffraction artefact): the grey values just outside the sample were lower than the background air, whereas the grey values just inside the sample where higher than the matrix gray values (see Figure S3). This surface feature was corrected with algorithm described in the surface feature correction section below. Otherwise, image preprocessing and image analysis were very similar as for the dog bone samples, that is, small scale noise was removed from the images by 3D gaussian filtering ($\sigma_i = 1$) and different materials (matrix, cowpea, pores) were separated using thresholding. Film top and bottom

surfaces were determined using algorithm defined in.[2] Volume fractions are calculated similarly as for dog bone samples except that only the voxels between the top and bottom surfaces were considered, when determining the number of voxels belonging to material A or the total number of voxels of the sample. The 3D visualizations of the film samples are given in Figure S4.
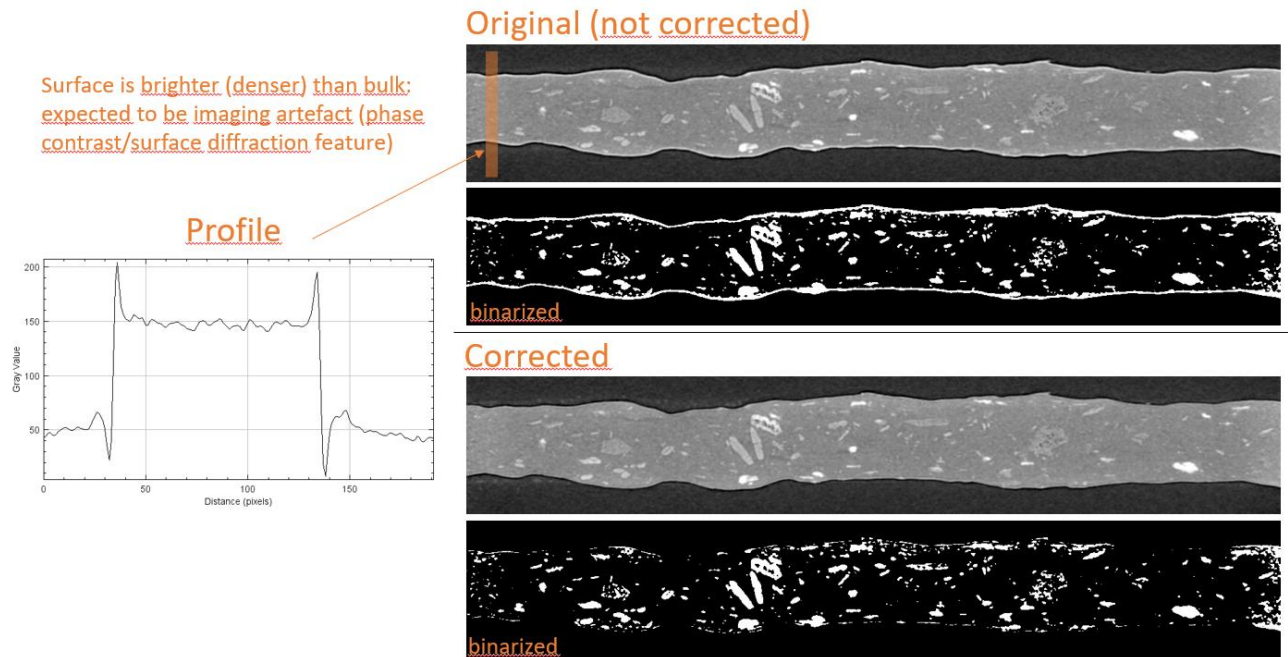
Figure S3: Surface artefact in X-ray tomography of bio-composite films containing 10 % cowpea sidestream as seen in slice image before (original) and after surface feature corrections (corrected). Grey scale on top and binarized i.e. threshold (fiber material) image bottom. Shown is also grey value profile from a small section of the original image.
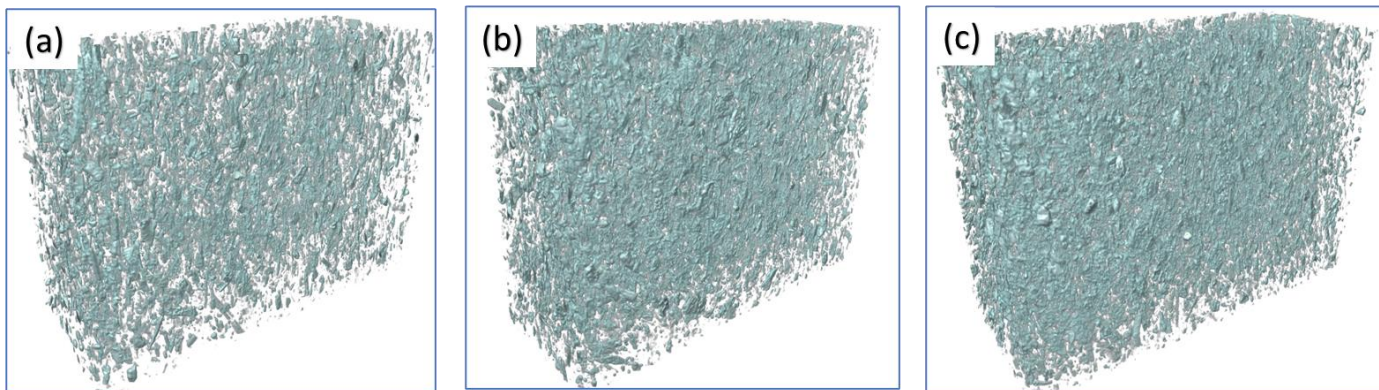
Figure S4: 3D visualizations of the fibres in the bio-composite films containing (a) 10, (b) 20 and (c) 30% cowpea sidestream. Polymer matrix not included, i.e. transparent.

Surface feature correction

Film surface region is corrected using following method. Grey values just outside the sample are slightly enhanced while just inside the sample the grey valu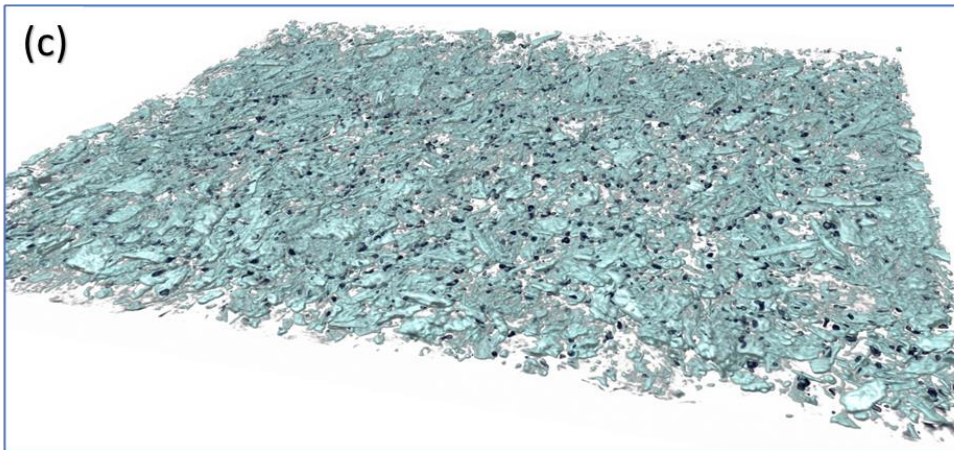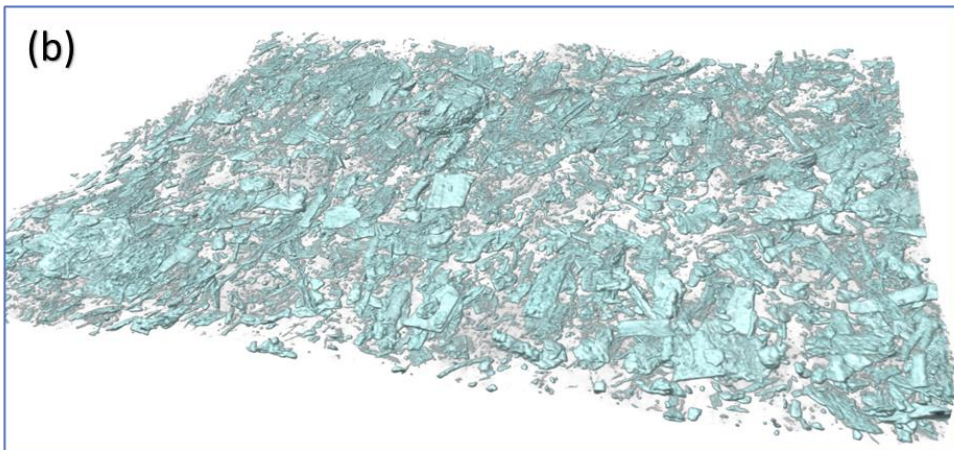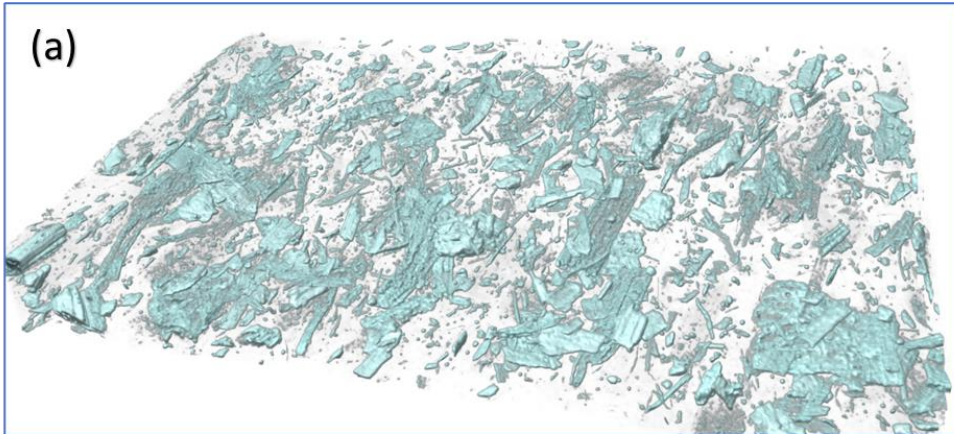es are slightly reduced. This is done by using gamma distribution function and dilation and erosion operations utilizing the following schematic algorithm:

```
#==================================================================
==================== #Surface feature correction algorithm
#==================================================================
====================
```

#separate and binarize the sample from background

binary_Image_help = threshold(Image)

#note: for samples which contain holes, these should be filled (to prevent "correction" of hole surface regions) at this point.

mask = 0   #initilize mask image. Should be same size as Image.

#make surface correction for outside region

for i from 0 to depth_out -1

   extrema_Image = dilated(binary_Image_help)   #dilate with one voxel layer

   gamma_Image = (extrema_Image – binary_Image_help)*w_out*gamma_norm(i,shape_out,scale_out)

   binary_Image_help = extrema_Image

   mask = mask + gamma_Image

#clean image arrays

clear extrema_Image, gamma_Image

#reinitialize binary image

binary_Image_help = threshold(Image)

#make surface correction for inside region

for i from 0 to depth_in

extrema_Image = erosion(binary_Image_help)   #erode with one voxel layer

gamma_Image   =   (binary_Image_help   -
extrema_Image)*w_in*gamma_norm(i,shape_in,scale_in)

binary_mask = extrema_Image

mask = mask + gamma_Image

#make surface correction

surface_corrected_image = (1 + mask)*Image

#===
====================

In above w_in, w_out are weight factors and normalized gamma distribution (gamma_norm)
is

$$g_N(x, k, \theta) = \frac{1}{N} g(x, k, \theta),$$

where gamma distribution is

$$g(x, k, \theta) = \frac{1}{(k-1)! \theta^k} x^{k-1} e^{-x/\theta},$$

and the normalization factor N is the maximum value of $g(x, k, \theta)$ at range x =[0,depth_in/out
-1]. Normalization guarantees that $g_N(x, k, \theta)$ can get at maximum value of one.

Algorithm parameter values used in the analysis were: depth_out = depth_in = 5, shape_out =
shape_in = 2, scale_out = scale_in = 1, w_out = 0.25, and w_in = -0.25.

References

[1] https://github.com/arttumiettinen/pi2

[2] Turpeinen et al. "Interface Detection Using a Quenched-Noise Version of the Edwards-
Wilkinson Equation", IEEE TRANSACTIONS ON IMAGE PROCESSING, VOL. 24, NO.
12, DECEMBER 2015, doi: 10.1109/TIP.2015.2484061